



Mechanical and Morphological Properties of 3D Printed Scaffold for Tissue Engineering Application

Muhammad Azmin Wafi Mohammed Noor, Abdul Manaf Abdullah*, Abdul Halim Abdullah, Solehuddin Shuib, and Zulkifli Abdul Ghaffar

School of Mechanical Engineering, College of Engineering, Universiti Teknologi MARA,
40450 Shah Alam, Selangor, Malaysia
abdulmanaf@uitm.edu.my

Abstract. Currently available designs for tissue engineering scaffold often focus on a structure that mimics the extracellular matrix while ignoring the mechanical properties needed for load bearing. This study aims to overcome the problems of existing scaffold designs by introducing new biologically and mechanically relevant scaffold designs for bone tissue. To reach these goals, new scaffold designs embedded with square, circular and hexagonal pores at three different pore sizes of 0.25, 0.30 and 0.35 were prepared using computer aided design (CAD) software. Their mechanical properties were modeled, and the physical and mechanical properties of the 3D-printed scaffolds were evaluated. Two materials, including PLA and acrylic resin were used to 3D print the scaffolds to ensure accurate control over the scaffold's structure and porosity. The mechanical properties of the scaffolds with three different pore sizes of 0.25, 0.30 and 0.35 mm were analysed using finite element analysis (FEA) and experimental testing. The results showed that the cubic design with circular pores displays the highest stress and strain values. The simulations indicate stress levels of 189.76 MPa and strain values of 9.4983%. Experimentally, it indicates stress values of 71.589 MPa and strain values of 58.92%. These values exceed those of the cubic designs with hexagonal and square pores. The results show that the proposed scaffold designs meet both biological and mechanical requirements, therefore contributing to the development of enhanced bone tissue engineering.

Keywords: scaffold design, bone tissue engineering, 3D print, DentaMODEL

1 Introduction

Bone defects caused by trauma, tumors, infections, or surgery may regenerate naturally, but certain significant defects may require clinical intervention for proper healing [1]. Bone tissue engineering seeks to repair bone defects by transplanting scaffolds into the affected area, therefore facilitating the replacement of scaffold materials with newly formed bone tissues within the body. The most effective scaffolds should contain ideal physical and biological properties

© The Author(s) 2024

N. A. S. Abdullah et al. (eds.), *Proceedings of the International Conference on Innovation & Entrepreneurship in Computing, Engineering & Science Education (InvENT 2024)*, Advances in Computer Science Research 117, https://doi.org/10.2991/978-94-6463-589-8_53

that promote cell adhesion, blood vessel growth, and nerve development for efficient clinical use [2]. In recent years, researchers have focused on improving the function of tissue-engineered constructions. This change involved the creation of implants that are infused with cells to match the structure of the existing tissues [3].

In tissue engineering, various methods, including solvent casting/particulate leaching, emulsion freeze-drying, phase separation, and electrospinning, are used to create scaffolds. However, these methods do not provide precise control over the size and shape of the pores. On the other hand, three-dimensional (3D) printing enables accurate control of structures, such as size, shape, and porousness, which improves the production of scaffolds used for tissue healing and regrowth [4]. The developing technology of (3D) printing has facilitated fast manufacturing of scaffolds with accurately controlled geometric forms and pore distribution [5]. The use of 3D printers enables smooth implementation of computer assisted approaches in creating tissue engineering scaffolds. Currently, various 3D printing methods are used for tissue engineering purposes, enabling the production of scaffolds using different materials like polyesters, ceramics, metals, and hydrogels [6].

The physical properties of the scaffold in tissue engineering are important, and its mechanical properties must be compatible with those of the implantation site. A scaffold that is very soft may experience deformation due to being compressed by native tissues that are close to it, which ultimately results in the scaffold losing its fundamental shape [7]. The compressive strength of cancellous bone is around 4 to 12 MPa meanwhile for cortical bone is around 130 to 180 MPa [8]. When designing scaffolds, it is important to properly consider multiple factors such as mechanical properties, porosity, and biocompatibility. It should be noted that enhancing certain properties might potentially result in unintended effects on a different property [9].

The requirement for successful tissue engineering scaffold lies on its mechanical and physical properties, with porosity being an essential requirement [9]. The amount of pores in scaffolds, or porosity, is important because it determines the adhesion of cells, the deposition of extracellular matrix, the entry of nutrients and oxygen, the discharge of metabolites, and the ingrowth of blood vessels and nerves [10]. High porosity can complicate the structure of scaffolds and decrease mechanical strength. An ideal pore size for bone tissue engineering is between 0.2 and 0.35 mm [11]. 3D printing can produce accurate scaffolds with The Young's modulus of structures ranging from 28 to 93 MPa, depending on their architecture [11]. However, bone implants are typically made from a simple shape and architecture which often mismatched with the natural bones' appearances and properties [12]. In some circumstances, the shape of the defect requires more complex scaffold designs as compared to standard circular or square shapes. However, the difficulties involved in constructing continuous printing paths for these complex designs have led researchers to concentrate on using simple circular or square setups with different deposition patterns, such as 0-90°, 0-45°, and 0-60°-120°. It is worth mentioning that the complex shape of scaffold enhances their efficacy in treating bone defects as compared to standard lay-down patterns of 0-90° and 0-45° [13]. Complex scaffold designs increase mechanical strength by optimizing load distribution, improving mechanical characteristics, and adjusting porosity, connection, and multifunctionality [14].

In this study, scaffolds with circular, square and hexagonal pores were created using computer aided design software. Each of the scaffold's were equipped with different pore sizes of 0.25, 0.30 and to 0.35 mm. Finite element analysis and actual testing were performed to understand the mechanical properties of the scaffolds. The physical characteristics of selected 3 D printed scaffolds were also observed. In this study, polylactic acid (PLA) and acrylic based resin were selected due to their biodegradability and compatibility for tissue engineering application. The use of 3D printing allows for precise control over scaffolds' structures, including size, shape, and porosity. The study also acknowledges the interconnected nature between printability of scaffolds using different nozzle diameters of fused deposition modeling (FDM) technique as well as the capability of digital light processing (DLP) technique towards fabricating a mechanically and biologically relevant scaffold for tissue engineering.

2 Material and Method

A scaffold prototype was planned and fabricated using Fused Deposition modeling (FDM), a widely used technology in additive manufacturing. This procedure involves the use of a thermoplastic filament that is heated to heat until it reaches its melting point, after which it is expelled in a series of layers to construct the scaffold structure [15]. The scaffold is also fabricated using the digital light processing (DLP) method, an additive manufacturing method that applies the photopolymerization technique. This process involves curing liquid photosensitive resin layer by layer using UV light [16].

2.1 Material

This study utilized two different materials, namely PLA (AA3D, Malaysia) and acrylic based resin (Asiga DentaModel, Asiga, Australia), to identify the ideal properties for the new scaffold design in tissue engineering. The PLA for 3D printing was in the form of filament with a diameter of 1.75 mm [17]. Meanwhile, the acrylic based resin was received in the form of a liquid form [18].

2.2 Scaffold design process

Three scaffolds with different designs were created using Catia V5 (Dassault Systems), a 3D design software that can be used for computer-aided design (CAD). The scaffold was designed using a three-dimensional cubic model with 6 mm x 6 mm x 6 mm dimensions. Figure 1 shows the scaffold design with hexagonal, circle and square pores. The pore sizes varied between 0.25, 0.30 and 0.35 mm, respectively. For bone tissue engineering, the optimal pore size of the scaffold is suggested to be between 0.2mm and 0.35mm. It is well documented that a 3D printer has the capability to create accurate structures by adding layers with the recommended pore size, resulting in well-connected pores and strong mechanical properties [11]. The scaffold designs with its pore sizes are summarized in Table 1.

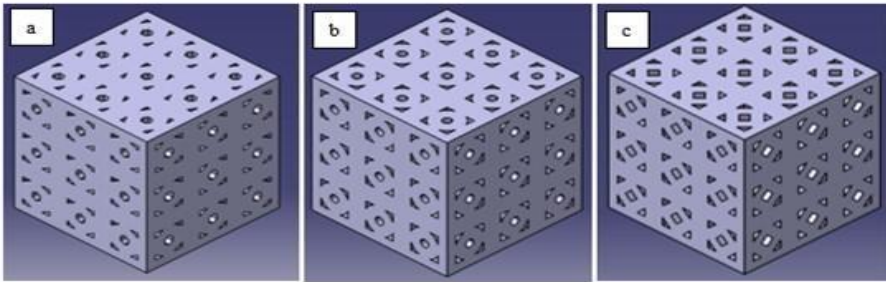


Fig. 1. CAD models for the scaffolds with pores. **a** hexagon, **b** circle, and **c** square

Table 1. Determined pore pattern and sizes for scaffold design

Pore patterns	Pore sizes (mm)
Hexagonal	0.25
	0.30
	0.35
Circular	0.25
	0.30
	0.35
Square	0.25
	0.30
	0.35

2.3 3D printing

The designed scaffolds were printed using an FDM 3D printer (Ender 3, Creality, China) at a temperature of 200°C, with a build plate temperature of 50°C and a constant printing speed of 30 mm/s. Regarding issues such as warping, printing cooling was activated to ensure that each layer cools sufficiently before the next layer was deposited, promoting better adhesion and reducing the likelihood of deformities. Table 2 shows the parameters for the 3D printing process. The 3D printing was conducted using three different nozzles of 0.1, 0.2 and 0.3 mm. In order to observe the printability of the scaffold using FDM techniques, scaffold with the biggest pore size of 0.35 mm was selected for the purpose. The scaffold was also printed using Digital light processing (DLP) with 385 nm 3D printing (MAX UV, ASIGA, Australia). The reference model's STL file was loaded into the Asiga MAX UV slicing programme (Asiga Composer, Asiga, Australia). The slicing programme was used to align the model horizontally at 0 degrees, with the model base directly on the build platform. The heated build platform temperatures were set at 60°C The resolution along the z-axis was determined and standardised at 50 µm [19].

Table 2. FDM 3D printing parameter

3D printing parameter	Value
Orientation	x-y
Printing speed	80 mm/s
Nozzle temperature	200 °C
Build plate temperature	50 °C
Infill density	100%
Layer height	0.2 mm
Wall thickness	0.8 mm
Top/bottom Thickness	0.8 mm
Print cooling	Yes
Built plate adhesion type	Skirt

2.4 Characterization of scaffolds

Physical properties

The 3D printed scaffold was examined using a scanning electron microscope (SEM, JSM-7600F, JEOL, Japan) to evaluate the architecture and surface morphology. The scaffolds were coated and image 15 kV voltage under a vacuum [1]. An optical microscope (BX60, Olympus, Japan) was also used to examine the scaffold. These scaffolds were placed on glass slides to improve the visibility of the microstructural characteristics. The optical microscope is equipped with a built-in digital camera allowing for taking high-resolution pictures.

Mechanical properties

The Universal Testing Machine (UTM) (servo pulser, Shimadzu, Japan) was employed to assess the compressive properties of 3D-printed specimens. The testing of 3D-printed scaffolds was conducted at a test speed of 1 mm/min.

Finite Element Analysis

The designed scaffold was subjected to meshing using tetrahedral elements, and it was used to replicate stress-strain interactions through finite element analysis with ANSYS (ANSYS Inc.). The finite element analysis simulations are conducted using the same methods as the experiments with the load of 400N. The boundary conditions consist of a rigid bottom and a compression load applied to the top [20].

3 Result and Discussion

3.1 Printability of scaffolds using different nozzles

The FDM printability was evaluated by testing three nozzle sizes of 0.1 mm, 0.2 mm, and 0.3 mm. The selection of nozzle diameter directly impacts the resolution, structural integrity, and overall performance of the scaffold. Smaller diameters allow for more precision and finer details but at the cost of longer printing times and greater risks of clogging. In contrast, greater diameters enable quicker printing while losing precision [21]. The 3D printer frequently encountered difficulties extruding the filament properly when using the 0.1 mm nozzle, resulting in failed prints and interruptions. Despite successful extrusion, the flow showed inconsistency, leading to failure in printing. The 0.2 mm nozzle produces excellent outcomes, providing an ideal precision. This nozzle size allows for the creation of high-resolution prints that possess fine details and smooth surfaces, making it perfect for complex models and designs. Furthermore, it presents fewer chances of blockage in comparison to the 0.1 mm nozzle. The 0.3 mm nozzle provides a balanced approach, combining detail and speed. Its larger size reduces the likelihood of clogging compared to the smaller nozzles, resulting in more reliable and consistent printing. The detailed result is as follows in Table 3.



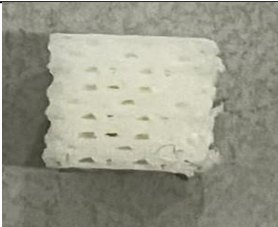

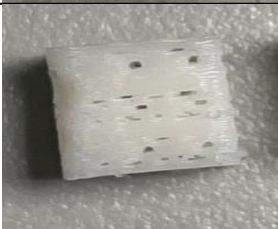
3.2 Morphological observation via microscopes

The scaffold, printed with a pore size of 0.35 mm and a hexagonal pattern, was chosen for detailed analysis using an optical microscope and Scanning Electron Microscopy (SEM) to confirm its match to the desired design. The choice to select a bigger pore size was caused by the practical advantage of an easier fabrication process resulting from decreased complexity. Upon initial observation using an optical microscope (Fig. 2a), the expected hexagonal shape was not visible in the scaffold. However, a clear proof of a hexagonal structure was revealed upon closer examination using scanning electron microscopy (SEM) (Fig. 2b). However, in spite of these findings, the scaffold did not demonstrate flawless matching with the desired design, indicating incapability of FDM to print structures embedded with micropores.

3.3 Scaffold Printing using Direct Light Processing Technique

Direct light processing (DLP) is an advanced 3D printing technique with many advantages compared to Fused Deposition Modelling (FDM). When problems arise with FDM, such as precision or surface finish limitations, switching to

Table 3. Nozzle size and printing result

Nozzle size	Nozzle	Printing result
0.1		Printing failed
0.2		
0.3		

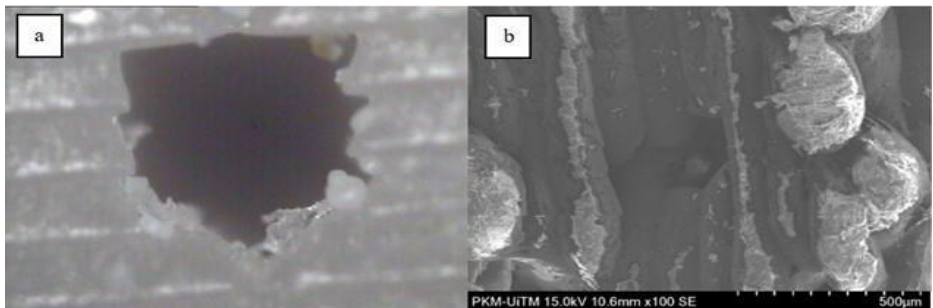


Fig. 2. Pore shape analysis using **a** Optical microscope and **b** SEM.

DLP and using materials like acrylic based resin can significantly improve the printed scaffold [22]. Acrylic based resin of DentaMODEL is an excellent option for producing precise and detailed scaffolds because it was created especially for high-resolution dental applications. In contrast to the layer-by-layer deposition technique of FDM, DLP uses a digital light projector to cure an entire resin layer all at once [23]. In addition, DentaMODEL resin provides improved mechanical qualities and biocompatibility, making it suited for use in the medical and dental fields. The formulation ensures that the printed scaffolds possess the strength and durability required to endure clinical use. Moreover, the material's biocompatibility guarantees secure and harmless contact with biological tissues, which is essential for any scaffold designed for medical applications. DentaMODEL is a dependable option for switching from FDM to DLP to produce complex, sturdy scaffolds. Figure 3 shows the scaffold printed with DentaMODEL. Based on this scaffold, the printing looks finer than the printing using FDM. The pore shape prints better using DLP.

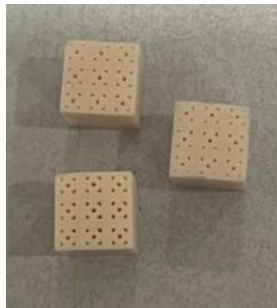


Fig. 3. Scaffold printed using DentaMODEL

3.4 Mechanical Properties

The compressive stress for each pore size has been demonstrated in Table 4. Due to their different geometries, pores of circle, hexagon, and square shapes show different compressive stress. Circle pores consistently show exceptional mechanical performance, with a maximum stress of 71.589 MPa when the pore size is 0.25mm. Their symmetrical shape allows for an even distribution of stress over the material, resulting in this feature. Circle pores improve the material's capacity to endure larger loads without deformation or failure by reducing stress concentrations [24]. On the other hand, hexagon pores demonstrate moderate peak stress levels, reaching a maximum of 59.768 MPa under similar conditions. Although hexagon structures transfer stress equally, they may have slightly higher concentrated stress at the corners than circular pores. This aspect can restrict their maximum stress capacity and overall mechanical durability compared to a circle. On the contrary, square-shaped pores consistently exhibit the lowest peak stress values compared to the other two shapes, reaching a maximum of 26.171 MPa at a pore size of 0.25mm. The presence of sharp corners in the square shape increases stress concentrations, significantly reducing its structural integrity and load-bearing capacity.

Table 4. Experiment Stress and Strain Value

Pattern design	Pore size (mm)	Stress (MPa)	Strain (%)
Cubic with hexagon	0.25	59.768 ±0.499	43.342 ±0.871
	0.30	38.515 ±1.430	34.721 ±0.968
	0.35	27.986 ±1.018	38.068 ±0.845
Cubic with circle	0.25	71.589 ±1.458	53.614 ±1.147
	0.30	48.181 ±0.907	43.372 ±0.831
	0.35	45.129 ±1.985	41.534 ±1.280
Cubic with square	0.25	26.171 ±1.270	40.022 ±0.896
	0.30	21.736 ±2.112	44.757 ±3.635
	0.35	25.244 ±1.058	46.404 ±0.851

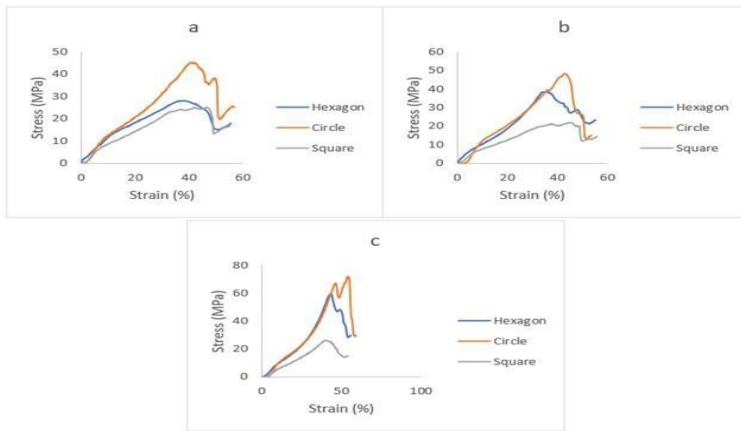


Fig. 4. Stress strain curve with different pore size. a 0.35mm, b 0.30mm, and c 0.25mm

The stress-strain graphs in Fig. 4 illustrate the mechanical behavior of materials that have different pore shapes, such as hexagon, circle, and square, with pore diameters of 0.35mm, 0.30mm, and 0.25mm. Materials with hexagon pores show a consistent increase in stress with strain up to a peak and then decrease, showing high stress sustainability before failing. On the contrary, circle pores show a more drastic increase in stress, reaching a greater peak and then decrease, showing their superior ability to withstand stress. Square pores reveal the least resistance to stress among the shapes, following a pattern like hexagons but with a lower peak. Circle-shaped pores consistently display higher peak stress values across all pore diameters, while square-shaped pores display the lowest. Hexagon pores display mid range values. Furthermore, there is a correlation between smaller pore sizes and greater stress values, which suggests that the shape and size of the pores have a significant impact on the stress-strain behavior of the material. The pore size of the material has an impact on its compressive strength [25]. In general, circle patterns and smaller pores are associated with higher stress responses.

3.5 Finite Element Analysis

The mechanical testing of the design scaffold with DentaMODEL was analysed using ANSYS. Figure 5 illustrates the outcomes of the specimen testing postapplication of load. In this figure, the behavior of the cube under the static structural analysis reveals how stress is distributed throughout the material when subjected to external loads. The color gradient inside each cube highlights areas of varying stress levels, with blue representing low stress and red indicating high stress. This distribution pattern shows that certain regions of the cube are more loaded than others. For instance, the green color in Fig. 3 is the spot where the scaffold is experiencing the highest stress, suggesting these regions are under significant strain and are more likely to deform or fail. In contrast, the blue areas signify regions of lower stress, indicating that these parts of the cube are less affected by the applied loads. Fig. 5(c) shows that the structure has the most green color compared to Fig. 5(a) and 5(b). The scaffold design of cubic with square pores most likely to fail with low compressive stress as compared to the hexagonal and circular pores.

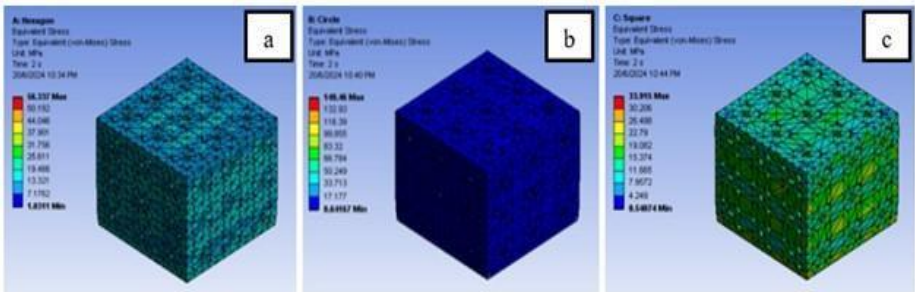


Fig. 5. Finite element analysis of scaffold design. **a** Hexagon, **b** Circle, and **c** Square

Table 5 shows the simulated maximum stress and strain of various designed scaffolds. The simulated elastic behavior of the scaffolds accurately reflects the physical behavior for strain values below 10%. The simulations were based on an isotropic elastic property model, leading to a linear increase in scaffold deformation with increasing compression force [26]. However, after the compression stress exceeds the yield stress, plastic deformation becomes the main factor, explaining the differences observed between the experimental and numerical results. The simulation results indicate that the maximum compressive stress is 189.76 MPa, followed by a strain of 9.3983%.

Table 5. Simulation stress and strain value

Design	Pore size (mm)	Stress (MPa)	Strain (%)
Cubic with hexagonal pores	0.25	59.990	3.072
	0.30	56.337	2.918
	0.35	51.836	2.899
Cubic with circular pores	0.25	189.760	9.498
	0.30	149.460	8.606
	0.35	92.425	5.742
Cubic with square pores	0.25	32.600	1.942
	0.30	33.915	2.101
	0.35	40.442	2.226

4 Conclusion

The cube with a circular pores is superior to the hexagonal and square porous structure in terms of compressive stress. Validation was conducted on the unit cells to confirm that they are not affected by the mesh size, guaranteeing dependable results. Out of the three scaffold designs that have different pore sizes, the scaffold with a circular pore size of 0.25 mm showed the highest compressive stress. This is partly due to its shape, particularly structure that has no edges by which are able to support surrounding structure. To summarize, using a circular pore design with the smallest pore size is a successful approach for creating new scaffolds with strong mechanical properties and good porosity. This combination is postulated to improve the biocompatibility of the scaffold.

Acknowledgment

Authors greatly acknowledged assistance from SIRIM Berhad for the 3D printing process.

References

1. Büyük, N.I., Aksu, D., and Torun Köse, G.: Effect of different pore sizes of 3D printed PLA-based scaffold in bone tissue engineering. *Int. J. Polym. Mater. Po.* 72(13), 1021–1031 (2023). doi:10.1080/00914037.2022.2075869
2. Su, X., Wang, T., and Guo, S.: Applications of 3D printed bone tissue engineering scaffolds in the stem cell field. *Regen. Ther.* 16, 63–72 (2021). doi.org/10.1016/j.reth.2021.01.007
3. Mani, M.P., Sadia, M., Jaganathan, S.K., Khudzari, A.Z., Supriyanto, E., Saidin, S., Ramakrishna, S., Ismail, A.F., and Mohd Faudzi, A.A.: A review on 3D printing in tissue engineering applications. *J. Polym. Eng.* 42(3) 243–265 (2022). doi:10.1515/polyeng-2021-0059
4. Belaid, H., Nagarajan, S., Barou, C., Huon, V., Bares, J., Balme, S., Miele, P., Cornu, D., Cavailles, V., Teyssier, C., Bechelany, M.: Boron Nitride Based Nanobiocomposites: Design by 3D Printing for Bone Tissue Engineering. *ACS Appl. Bio. Mater.* 3(4), 1865–1874 (2020). doi.org/10.1021/acsabm.9b00965
5. Gao, Q., Xie, C., Wang, P., Xie, M., Li, H., Sun, A., Fu, J., He, Y.: 3D printed multi-scale scaffolds with ultrafine fibers for providing excellent biocompatibility. *Mater. Sci Eng. C* 107, 110269 (2020). doi:10.1016/j.msec.2019.110269
6. Zaszczynska, A., Moczulska-Heljak, M., Grady, A., and Sajkiewicz, P.: Advances in 3D printing for tissue engineering. *Materials* 14(12), 3149 (2021). doi:10.3390/ma14123149
7. Germain, L., Fuentes, C.A., van Vuure, A.W., des Rieux, A., and Dupont-Gillain, C.: 3D-printed biodegradable gyroid scaffolds for tissue engineering applications. *Mater. Design* 151, 113–122 (2018). doi:10.1016/j.matdes.2018.04.037
8. Yang, S., Leong, K.-F., Du, Z. M. E., and Chua, C.-K.: The design of scaffolds for use in tissue engineering. Part I. Traditional factors. *Tissue Eng.* 7(6), 679–89 (2001). doi:10.1089/107632701753337645
9. Shirzad, M., Zolfagharian, A., Matbouei, A., and Bodaghi, M.: Design, evaluation, and optimization of 3D printed truss scaffolds for bone tissue engineering. *J. Mech. Behav. Biomed.* 120, 104594 (2021). doi.org/10.1016/j.jmbbm.2021.104594
10. Wu, T., Yu, S., Chen, D., and Wang, Y.: Bionic design, materials and performance of bone tissue scaffolds. *Materials* 10(10), 1187 (2017). doi:10.3390/ma10101187
11. Gregor, A., Filová, E., Novák, M., Kronek, J., Chlup, H., Buzgo, M., Blahnová, V., Lukášová, V., Bartoš, M., Nečas, A., and Hošek, J.: Designing of PLA scaffolds for bone tissue replacement fabricated by ordinary commercial 3D printer. *J. Biol. Eng.* 11, 31 (2017). doi:10.1186/s13036-017-0074-3
12. Li, Z., Wang, Q., and Liu, G.: A Review of 3D Printed Bone Implants. *Micromachines-Basel.* 13(4) 528 (2022). doi:10.3390/mi13040528
13. Fallah, A., Altunbek, M., Bartolo, P., Cooper, G., Weightman, A., Blunn, G., Koc, B.: 3D printed scaffold design for bone defects with improved mechanical and biological properties. *J. Mech. Behav. Biomed.* 134, 105418 (2022). doi:10.1016/j.jmbbm.2022.105418
14. Kolken, H.M.A., Garcia, A.F., Du Plessis, A., Rans, C., Mirzaali, M.J., and Zadpoor, A.A.: Fatigue performance of auxetic meta-biomaterials,” *Acta Biomater.* 126, 511–523 (2021) doi:10.1016/j.actbio.2021.03.015
15. Söhling, N., Neijhoft, J., Nienhaus, V., Acker, V., Harbig, J., Menz, F., Ochs, J., Verboket, R.D., Ritz, U., Blaeser, A., Dörsam, E., Frank, J., Marzi, I., and Henrich, D.: 3D-printing of hierarchically designed and osteoconductive bone tissue engineering scaffolds. *Materials* 13(8), 1836 (2020). doi:10.3390/MA13081836

16. Ribrant, A.O and Eklund, M.: Bio-based resins for digital light processing: Mechanical and degradable properties. B. Tech. Thesis, School of Industrial Technology and Management (ITM), KTH Royal Institute of Technology (2023).
17. Baptista, R. and Guedes, M.: Morphological and mechanical characterization of 3D printed PLA scaffolds with controlled porosity for trabecular bone tissue replacement. *Mater. Sci. Eng. C* 118, 111528 (2021). doi:10.1016/j.msec.2020.111528
18. Sayed, M.E., Lunkad, H., Mattoo, K., Jokhadar, H.F., AlResayes, S.S., Alqahtani, N.M., Alshehri, A.H., Alamri, M., Altowairqi, S., Muaddi, M. and Huthan, H.M.: Evaluation of the effects of digital manufacturing, preparation taper, cement type, and aging on the color stability of anterior provisional crowns using colorimetry. *Med. Sci. Monit. Basic Res.* 29, e941919 (2023), doi:10.12659/MSMBR.941919
19. Lin, L.H., Granatelli, J., Alifui-Segbaya, F., Drake, L., Smith, D. and Ahmed, K.E.: A proposed in vitro methodology for assessing the accuracy of three-dimensionally printed dental models and the impact of storage on dimensional stability. *Appl. Sci.-Basel.* 11(13) 5994 (2021). doi:10.3390/app11135994
20. Jin, Y., Xie, C., Gao, Q., Zhou, X., Li, G., Du, J. and He, Y., 2021. Fabrication of multi-scale and tunable auxetic scaffolds for tissue engineering. *Mater. Design* 197, 109277 (2021). doi:10.1016/j.matdes.2020.109277
21. Triyono, J., Sukanto, H., Saputra, R.M. and Smaradhana, D.F.: The effect of nozzle hole diameter of 3D printing on porosity and tensile strength parts using polylactic acid material. *Open Eng.* 10(1), 762-768 (2020). doi:10.1515/eng-2020-0083
22. Li, H., Dai, J., Wang, Z., Zheng, H., Li, W., Wang, M. and Cheng, F.: Digital light processing (DLP)-based (bio) printing strategies for tissue modeling and regeneration. *Aggregate* 4(2), e270 (2023). doi:10.1002/agt2.270
23. Liang, H., Wang, Y., Chen, S., Liu, Y., Liu, Z. and Bai, J. Nano-hydroxyapatite bone scaffolds with different porous structures processed by digital light processing 3D printing. *Int. J. Bioprint.* 8(1), 198–210 (2022). doi.org/10.18063/ijb.v8i1.502
24. Kang, J.H., Sakthiibirami, K., Jang, K.J., Jang, J.G., Oh, G.J., Park, C., Fisher, J.G. and Park, S.W., 2022. Mechanical and biological evaluation of lattice structured hydroxyapatite scaffolds produced via stereolithography additive manufacturing. *Mater. Design* 214, 110372 (2022). doi:10.1016/j.matdes.2021.110372
25. Jahir-Hussain, M.J., Maaruf, N.A., Esa, N.E.F. and Jusoh, N.: The effect of pore geometry on the mechanical properties of 3D-printed bone scaffold due to compressive loading. *IOP Conf. Ser.: Mater. Sci. Eng.* 1051, 012016 (2021). doi:10.1088/1757-899X/1051/1/012016
26. Xu, Z., Omar, A.M. and Bartolo, P.: Experimental and numerical simulations of 3D-printed Polycaprolactone scaffolds for bone tissue engineering applications. *Materials* 14(13), 3546 (2021). doi:10.3390/ma14133546

Open Access This chapter is licensed under the terms of the Creative Commons Attribution-NonCommercial 4.0 International License (<http://creativecommons.org/licenses/by-nc/4.0/>), which permits any noncommercial use, sharing, adaptation, distribution and reproduction in any medium or format, as long as you give appropriate credit to the original author(s) and the source, provide a link to the Creative Commons license and indicate if changes were made.

The images or other third party material in this chapter are included in the chapter's Creative Commons license, unless indicated otherwise in a credit line to the material. If material is not included in the chapter's Creative Commons license and your intended use is not permitted by statutory regulation or exceeds the permitted use, you will need to obtain permission directly from the copyright holder.

